Modeling of the spatial structure by means of wide-angle x-ray scattering and extended x-ray-absorption fine structure for the $Cu_8As_{26}Se_{66}$ and $Cu_{26}As_{37}Se_{37}$ semiconductor alloys

D. Gomez-Vela
Departamento de Ingenieria Electrica y Electrónica, Escuela Universitaria Politécnica de Cádiz, Universidad de Cadiz, 11003 Cádiz, Spain

L. Esquivias
Departamento de Estructura y Propiedades de los Materiales, Facultad de Ciencias, Universidad de Cádiz, Apartado 40, Puerto Real (Cádiz), Spain

C. Prieto
Instituto de Ciencia de Materiales de Madrid (sede B), Consejo Superior de Investigaciones Científicas, Universidad Autónoma (C-4), 28049 Madrid, Spain
and Laboratoire pour l'Utilisation du Rayonnement Electromagnetique, 91405 Orsay Cedex, France
(Received 6 April 1992; revised manuscript received 28 June 1993)

Short-range orders of two amorphous alloys of the chalcogenide Cu-As-Se family have been studied by extended x-ray-absorption fine structure (EXAFS) and wide-angle x-ray scattering (WAXS). Up to now, the construction of spatial models by a modified metropolis Monte Carlo simulation technique carried out by us was solely based on the information gained in the WAXS experiments. In this work, we also take into account the information extracted from the spectroscopic EXAFS experiments to get more-realistic spatial models. In this way, the average coordination numbers of the three different atoms and their distances to the first coordination sphere have been determined in $Cu_8As_{26}Se_{66}$ and $Cu_{26}As_{37}Se_{37}$. The extraction of the inverse Fourier transforms to the generated atomic distribution function leads us to a simulated reduced interference function $si(s)$, in good agreement with its experimental counterpart.

I. INTRODUCTION

During the last few years amorphous semiconductors have been used in the manufacture of solar cells, batteries, and phototransistors[1] as well as in some steps of the technological processing of very-large-scale integration (VLSI) microelectronic circuits. Recently the chalcogenide family (CdS_xSe_{1-x}) appears to play an important role in the synthesis of materials with nonlinear optical properties made of a ceramic matrix and the dispersion within of a chalcogenide phase.[2] In this way, the structural study of these compounds has gained additional interest, as electronic properties are related to the glassy structure.

The addition of copper to amorphous As-Se alloy systems has been studied by many authors[3,4] and there result significant modifications of its properties, including the observation of a glass transition, network connectivity, and electrical conductivity. The last one strongly depends on short-range order[5] (SRO), and one of the main purposes of this work is to determine the distances and pair coordinations of each component. Experimentally, the metal atoms appear to be tetrahedrally coordinated,[3,6] and the general structural model proposed by Liu and Taylor[7] gives a tetrahedral structure when the metal is added to the glasses. The particular spatial models proposed in this work also satisfy this feature.

Wide-angle x-ray scattering (WAXS) is a mature technique.[8] A complete data analysis begins by obtaining the radial distribution function (RDF) that carries the global average structural parameters concerned with the first coordination shell, such as, the average distance between atoms pairs and the coordination number. This is related to the position and area of the first peak.

Extended x-ray-absorption fine structure (EXAFS) is a very useful technique to determine separately the coordination number for the three components. In this way the EXAFS experiments have been performed at the three absorption K edges corresponding to the Cu, As, and Se elements at room temperature. The availability of EXAFS spectroscopy has led to the determination of a set of parameters describing the SRO that also satisfies WAXS experiments, which has challenged us to construct dimensional models that include this information. This means that EXAFS could act as a way of testing and refining our previous Metropolis Monte Carlo (MC) simulation technique as a second local probe. The purpose is to reach more realistic and accurate models from a physical point of view.

II. EXPERIMENTAL

Selected samples were named L and H referring to their low or high copper concentration. Case L represents a deviation in the As/Se ratio of the widely studied composition Cu_x-$(As_2Se_3)_{1-x}$, while the other presents a higher Cu concentration and an As/Se ratio equal to 1. Both compositions are included in the amorphization region (see Borisova[9]).

Amorphous materials with the above-mentioned composition, were prepared by the usual melt-quenching technique. The glassy nature of the samples was confirmed by x-ray diffractometric scanning, showing the absence of the peaks, which are characteristic of crystalline phases. Figure 1 shows the corresponding diffractograms obtained with Cu-$K\alpha$ radiation ($\lambda=1.54$ Å). The material densities, measured by the pycnometric method, are 4.4 ± 0.2 g/cm^3 and 5.8 ± 0.2 g/cm^3 for samples L and H, respectively.

Standard WAXS experiments were performed on a Siemens D500 diffractometer equipped with a graphite monochromatic, scintillation counter and standard associated electronic equipment. Two sets of four series of intensities collected with Bragg-Brentano geometry in the angle interval $8°\leq 2\theta 110°$ for both Cu-$K\alpha$ and Mo-$K\alpha$ ($\lambda=0.71$ Å) radiation with a step size of $\Delta(2\theta)=0.2°$, were used from 8° to 70°, and $\Delta(2\theta)=0.5°$ from 70° to 110°. Counts were measured by keeping a fixed time interval for purposes of automatic data registration by means of Siemens Daco systems, ensuring in every case at least 4000 counts in each measured time interval. The intensity assigned to each observation point was the mean value of those series measured at that point. Most of the averaged values lie within 3% of the average with a maximum deviation of 5%.

EXAFS experiments were carried out on the beamline EXAFS-III at the DCI storage ring (Orsay) with an electron beam energy of 1.85 GeV and an average current of 250 mA. Data were collected with a fixed-exit monochromator using two flat Si(311) crystals in transmission mode. Detection was carried out using two ion chambers with air fill gas. The air pressure was selected in order to have a good signal-to-noise ratio and a good linearity; no significant changes have been observed in the Fourier transform of the EXAFS data when different thickness of the sample were measured. The fast EXAFS acquisition operative mode[10] was used to collect at least ten spectra in order to average them. The energy resolution was estimated to be about 2 eV by the Cu foil 3d near edge feature. The energy calibration was monitored using the Cu foil sample and was set at 8991 eV at the first maximum above the edge.

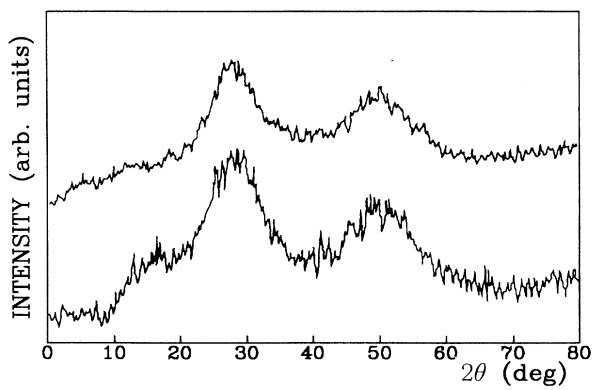

FIG. 1. X-ray diffractogram with Cu-$K\alpha$ radiation for $Cu_{26}As_{37}Se_{37}$ (above) and $Cu_8As_{26}Se_{66}$ (below) samples.

Samples were prepared by powdering, sieving, and then selecting particles smaller than 10 microns by floating the powder. The particles were then deposed on tape. About two layers of tape were used to make samples with $\Delta\mu x$ of 0.1–1.0 and a total μx less than 1.5.

III. ANALYSIS OF THE RESULTS

A. RDF from x-ray-scattering experiments

The observed intensities were corrected for background, polarization, and multiple scattering and were normalized into electron units (e.u.) by the high-angle method,[11] and, subsequently, the incoherent scattering was subtracted.

The RDF is calculated as follows:

$$4\pi r^2\rho(r)=4\pi r^2\rho_0+rG(r)\ , \tag{1}$$

where ρ_0 and $\rho(r)$ represent the mean atomic distribution and the local atomic density, respectively, and $G(r)$ stands for the Fourier transform of a function of experimental intensities, being

$$G(r)=\int_0^{\mathrm{SMAX}} F(s)\sin(sr)ds \tag{2}$$

with s being equal to the scattering vector modulus, and $F(s)$ being the interference function given by

$$F(s)=s\,\mathrm{i}(s)\ , \tag{3}$$

with i(s) being a function given by

$$\mathrm{i}(s)=\frac{I_{\mathrm{e.u.}}-\sum x_i f_i^2}{\left[\sum x_i f_i\right]^2}\ , \tag{4}$$

where x_i is the atomic fraction of the i element and f_i the atomic scattering factor with $i=$Cu, As, or Se, and $I_{\mathrm{e.u.}}$ represent the resulting intensity values in electronic units after correction.

The interference functions $F(s)$, were built up taking the Cu-$K\alpha$ data for the interval $0.57\leq s\leq 4.01$ Å^{-1} and those of Mo-$K\alpha$ for $4.01\leq s\leq 11.77$ Å^{-1} for the L sample. Similarly these limits are $0.57\leq s\leq 3.98$ Å^{-1} and $3.98\leq s\leq 11.67$ Å^{-1}, for the H sample. Then the data were theoretically extended by the method described by D'Anjou and Sanz[12] up to $s=30$ Å^{-1} to avoid spurious oscillations in $G(r)$ due to the cutoff. The RDF after the above-mentioned procedure is plotted in Fig. 2, for both samples.

The alloys under study were obtained in a second instance, and the entire experimental and numerical process was repeated up to the point of evaluating and comparing both RDF's. No difference has been observed between these two assays, increasing the confidence in the method's accuracy.

From the RDF point of view, the following information can be gathered: the limits of the first peak range in the L sample from 2.19 up to 2.59 Å, and for the H sample between 2.20 and 2.65 Å. The range does not allow us to reject any kind of bond between the different elements in the alloys, as all the standard bond distances are included in these limits. The first peak position for the

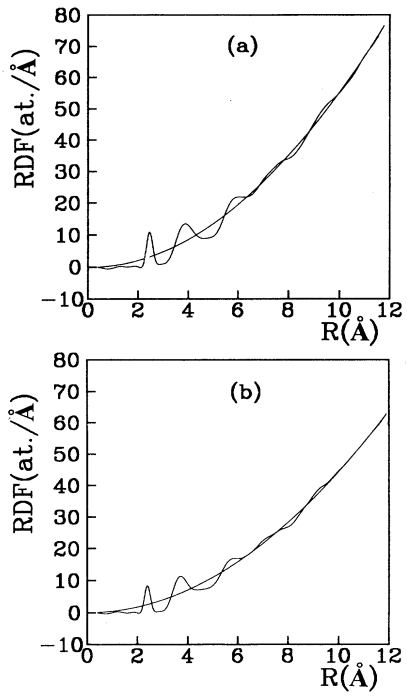

FIG. 2. Extended radial distribution function up to $r=12$ Å (a) for the $Cu_{26}As_{37}Se_{37}$ alloy and (b) for the $Cu_8As_{26}Se_{66}$ alloy.

low-Cu-concentration sample is 2.40 Å, and for the high-Cu-concentration sample it is 2.44 Å.

The area under the first peak represents the first-neighbors average coordination (i.e., the atomic network connectivity). The ideal average coordination value for covalent amorphous chalcogenides in the Phillips sense is 2.45 atoms[13] and the obtained value for the L sample is $A_{\mathrm{RDF}}(L)=2.54$ atoms. It indicates a slightly higher connectivity than in Ref. 14, representing an important deviation of the structure's covalent behavior. However, the value obtained for the H alloy $A_{\mathrm{RDF}}(H)=3.58$ atoms clearly indicates a high connectivity involving the presence of noncovalent bonds. On the other hand, the theoretical expression of the area under the first peak is

$$A=\frac{1}{\left(\sum x_i Z_i\right)^2}\sum_i\sum_j x_i Z_i Z_j n_{ij} \ , \tag{5}$$

where Z_i is the atomic number of element i and n_{ij} the average number of i-type atoms in the first coordination sphere of a j-type atom.

Taking into account the relationships for pair coordination in our ternary compounds

$$n_{ij}=n_{ji}\frac{P_i}{P_j} \ , \tag{6}$$

where i and j are Cu, As, or Se, and P_i and P_j are the percentages of each i and j component in the sample, the following equations for the area under the first peak for the L and H samples were obtained:

$$A=8.99(0.769n_{33}+0.583n_{23}+0.283n_{22}+0.158n_{13}+0.153n_{12}+0.067n_{11}) \ , \tag{7}$$

$$A=9.56(0.427n_{33}+0.823n_{23}+0.403n_{22}+0.513n_{13}+0.498n_{12}+0.219n_{11}) \tag{8}$$

with 1=Cu, 2=As, and 3=Se.

B. EXAFS spectra

The recordings of the absorption spectra at the K edge for the three components of $Cu_8As_{26}Se_{66}$ and $Cu_{26}As_{37}Se_{37}$ have been performed on samples with the same thickness, and has been reported previously.[15]

A classical procedure has been used to analyze the EXAFS spectrum. Above the edge, the background signal was removed by a multiple-iteration curve smoothing procedure. The analysis of the EXAFS signal to get the position of the neighbors around the absorbing atom has been carried out using the well-known EXAFS expression:[16]

$$\chi(k)=\sum_j \frac{N_j}{kR_j^2}\exp(-2k^2\sigma_j^2)\exp\left[-\Gamma_j\frac{R_j}{k}\right]f_j(k)\times\sin[2kR_j+\phi_j(k)] \ , \tag{9}$$

which describes the EXAFS oscillations for a Gaussian distribution of neighbors around the central atom, in the single scattering theory and in the plane-wave approximation. k is the wave vector of the photoelectron, which is related to the electron mass (m_e) and with the threshold energy (E_0) by

$$k=\left[\frac{2m_e}{\hbar^2}(E-E_0)\right]^{1/2} \ . \tag{10}$$

N_j is the average coordination number for the Gaussian distribution of distances centered at the R_j value; σ_j is the Debye-Waller contribution; $\phi_j=2\delta+\gamma_j(k)$ is the phase shift, with δ and γ_j being the central and backscattering atom phase shifts, respectively; $f_j(k)$ is the amplitude of the backscattering atoms; and Γ_j is related to the photoelectron's mean free path.

Data analysis has been carried out by comparing the filtered data with the EXAFS contribution calculated in the k and R spaces. After this interactive process, a standard minimization procedure has been applied in order to obtain the parameter that best fits the experimental data. The backscattering amplitude and phase functions were taken as the reported ones by Mckale *et al.*[17] Special attention has been paid to the coordination number in order to avoid the possible errors in the calculated amplitude function. First, we have fitted some crystalline samples[18] of these elements, and the fittings work correctly. These errors must coincide directly with N; in this way the relative coordination will be compatible with the stoichiometry of the sample and, moreover, we have additional data, which are the RDF obtained by WAXS in order to compare the mean coordination obtained from EXAFS.

The analysis shows that, like the conductivity, the Γ_j parameter (which is related to the photoelectron's mean free path) hardly changes from one compound to another. The Debye-Waller factors (σ_j^2) were taken in a first approximation for both samples, as were those obtained for the crystalline As_2Se_3, where the distances and coordination numbers are known, and their EXAFS signals have been analyzed in the same way. The Γ_j parameters were taken to be the same as the corresponding to crystalline $AsSe_3Ag$. The free parameters in the first step of the data fitting are the distance and coordination number for the two backscatterer neighbors, the changes in the threshold energy (ΔE_0) and the change in Debye-Waller factors.

Physically, each atom may be surrounded by three different types of atoms. In order to reduce the unknowns in Eq. (8), we have performed a first analysis[18] without making any distinction between As and Se as backscatterers, as the fitting program is unable to find a solution when working with such a high number of unknown parameters. This approximation is valid because of the proximity of As and Se in the Periodic Table. This leads to a set of n_{ij} and r_{ij}, for the best fitting parameters, which are presented in Table I, in the columns headed N and d, respectively.

The number of parameters (P) that can be obtained from the EXAFS measurements is given by $P=2\Delta k\Delta R/\pi$ taking into account the Nyquist criterion,[19] where Δk is the range to calculate the Fourier transform and ΔR is the range in R space used to perform the inverse Fourier transform. Values for those experiments are $\Delta k=11$ Å^{-1} and $\Delta R=1.2$ Å, which allow a number of parameters $P=8.4$. In Table I every EXAFS parameter is listed but not all of them are independent ones. Distances between two kinds of atoms must be the same independently from the absorption edge, from which they have been measured. On the other side, the mean free path factor Γ must be the same at every edge for each sample; thus, we have 5, 7, and 7 free parameters for $Cu_8As_{26}Se_{66}$ and 8, 7, and 7 free parameters for $Cu_{26}As_{37}Se_{37}$ (at the Cu, As, and Se absorption K edges, respectively) because we have taken only one Debye-Waller factor value per absorption-edge fitting.

Some remarks can be made about the coordination of the three kind of atoms. The average calculated coordinations, in the case of the Cu K-absorption edge are 3.96 and 3.99, similar to the value 4.0, as reported by Hunter *et al.*[20] For the As K edge the value of its mean coordination is 2.97 and 2.99 similar to the value of 3.0 obtained by means of the nuclear quadrupolar resonance (NQR) experiment reported by Saleh *et al.*[21] According to the formal valence shell (FVS) proposed by Liu[22] and Taylor in a compound such as $Cu_xAs_uSe_v$, with $x+u+v=1$, where n_m is the area under the first peak of the WAXS RDF, the averaged coordination for Se is

$$n_{\mathrm{Se,FVS}}=\frac{n_m-4x-3u}{v} . \tag{11}$$

For purposes of comparison, the Se average coordinations of both compounds were calculated by application of the FVS formulas resulting $n_{\mathrm{Se,FVS}}(L)=2.18$ and $n_{\mathrm{Se,FVS}}(H)=3.86$, which represents a better than 5% agreement with those obtained from EXAFS analyses, which are $n_{\mathrm{Se,EXAFS}}(L)=2.25$ and $n_{\mathrm{Se,EXAFS}}(H)=3.83$, respectively.

It should be noted that the resulting coordinations are compatible with the sample's stoichiometry, which may be interpreted as an autoconsistency test, since there was no *a priori* supposition on the coordination number. On the other hand, a good agreement is obtained by comparison of the mean coordination number and distances with those obtained from WAXS RDF of both samples. The mean coordination number can be directly obtained from the area under the first peak of WAXS RDF: $A_{\mathrm{RDF}}(L)=2.54$ and $A_{\mathrm{RDF}}(H)=3.58$ atoms. In combination with Eq. (11), they can be compared to those obtained by substituting data of Table I in the approximated equation of the area below the first peak [Eq. (5)], which gives $A_{\mathrm{EXAFS}}(L)=2.51$ and $A_{\mathrm{EXAFS}}(H)=3.6$.

C. Modeling technique

The procedure for building up a tridimensional model, generated from SRO information supplied by the WAXS RDF and implemented by MC simulation techniques was reported by Esquivias and Sanz,[23] and more recently by Vazquez *et al.*[24] We have modified the methodology to enable the inclusion of the constraint set supplied by the EXAFS experiments, and subsequently a comparison of

TABLE I. Fit results of EXAFS experiments for $Cu_8As_{26}Se_{66}$ and $Cu_{26}As_{37}Se_{37}$ alloys.

Sample	E_0 (eV)	Pair	ΔE_0 (eV)	N	d (Å)	σ^2 (Å)^2)	Γ (Å^{-2})
$Cu_8As_{26}Se_{66}$	8 976.0	Cu-Cu					
		Cu-(AsSe)	10.0	3.96	2.43	0.103	2.0
	11 857.6	As-Cu	2.0	0.11	2.46	0.062	2.0
		As-(AsSe)		2.86	2.40	0.064	
	12 646.0	Se-Cu	6.0	0.44	2.43	0.070	2.0
		Se-(AsSe)		1.81	2.39	0.066	
$Cu_{26}As_{37}Se_{37}$	8 977.0	Cu-Cu	2.0	0.29	2.50	0.080	2.0
		Cu-(AsSe)		3.70	2.39	0.109	
	11 857.0	As-Cu	0.0	0.66	2.41	0.060	2.0
		As-(AsSe)		2.33	2.41	0.075	
	12 646.0	Se-Cu	5.0	1.93	2.36	0.087	2.0
		Se(AsSe)		1.90	2.42	0.069	

TABLE II. Number of generated (P) and located (N) positions, with the indicated distributions of Cu, As, and Se atoms for the alloys L and H.

Sample	P	N	Cu atoms	As atoms	Se atoms
$Cu_8As_{26}Se_{66}$	475	252	20	66	166
$Cu_{26}As_{37}Se_{37}$	429	349	91	129	129

both procedures was carried out.

In any case the basic aim is the determination of the tridimensional model that verifies, as a necessary condition, the structural information experimentally obtained, and simultaneously satisfies, as much as possible, the known physicochemical properties of the material under study and its elements.

The basic steps in the modeling process are (i) generation of the initial model, (ii) calculation of its corresponding reduced RDF given by $rG_{\mathrm{mod}}(r)$, (iii) evaluation of the average quadratic deviation ε^2 between experimental and simulated reduced RDF, (iv) random relocation of selected atomic positions, (v) follow up of the model evolution, and (vi) obtaining the thermal factors and statistics of the best model.

Generation of the initial configuration consists of the saturation of a sphere of 12-Å radius with P spatial position (x_1,x_2,x_3) compatible with the bond distance and the angle determined by a random process, and the assignment of identity (Cu, As, or Se) to a set of N positions, by elimination of those with lower coordination.

N is the number of atoms that can be located inside the sample, and is a partition of Cu, As, and Se atoms, depending on the samples composition. The value of N is given by

$$N=\left[\rho_0\frac{A}{M_a}V\right], \tag{12}$$

where ρ_0 is the experimentally measured density, A is Avogadro's number, M_a is the atomic mass of the composition unit, and V is the volume of the simulated model.

Table II represents the values of P, N, and the distribution for every kind of atom in samples L and H, within a sphere volume of 12 Å of radii, and large enough to statistically represent the sample and small enough to be handled with a reasonable computational effort.

The model's reduced RDF is calculated by simulating its diffraction process, and then comparing it with the experimental sphere obtained by multiplying the reduced RDF, $rG_{\mathrm{exp}}(r)$, with the one proposed by Mason,[25] which takes into account the sample's finite extension and represents the probability of finding a distance r inside a sphere with a radius R, by means of the equation:

$$D(r)=1.0-1.5(r/2R)+0.5(r/2R)^3 . \tag{13}$$

From now on a displacement of $\Delta=0.5$ Å of a randomly selected specific atom and its direction are applied, and test if a reduction in the ε^2 occurs, while the remaining above-mentioned constraints are still satisfied. If this is the case, the movement is accepted and the cycle is repeated up to a moment where interactively a decrease in Δ is imposed due to very slow observed convergence of the process and extremely long computation time. This situation favored the follow up of the process until a $\Delta=0.1$ Å is applied and the system reaches a near steady state of convergence with a low ε^2 factor, given by the expression

$$\varepsilon^2=(1/M)\sum_{i=1}^{M}[r_iG_{\mathrm{exp}}(r_i)-r_iG_{\mathrm{mod}}(r_i)]^2 , \tag{14}$$

where the r_i's correspond to the M points sampled in the comparison. Table III gives the number M of valid movement, and the ε^2 reached, for every Δ step, in the samples L and H for the WAXS RDF procedure and for the combined WAXS-EXAFS method.

Once the value of $\Delta=0.1$ Å was completely exploited we did not decrease it again as the lower values have no physical meaning, since they are obscured by the thermal agitation. Next a refining of thermal factors was initiated. By the light of WAXS RDF, we define five coordination spheres, whose extreme radii depend on their own WAXS RDFS data (Table IV). Then starting with an initial thermal isotropic factor of $\sigma_0=0.1$ Å, a set of σ_j values (Table IV) was obtained, which best fits the simulated model reduced RDF to the experimental one, using

TABLE III. Positions refining process for WAXS method and combined WAXS+EXAFS method for each sample.

Sample	Δ (Å)	M	ε^2
$Cu_8As_{26}Se_{66}$		0000	3.3745
	0.5	0443	1.4461
(WAXS method)	0.4	1338	0.0933
	0.3	1435	0.0759
	0.2	1674	0.0470
$Cu_{26}As_{37}Se_{37}$		0000	3.7910
	0.5	0716	0.7289
(WAXS method)	0.4	1342	0.1489
	0.3	1558	0.0899
	0.2	1943	0.0392
	0.1	2214	0.0266
$Cu_8As_{26}Se_{66}$		0000	3.0441
	0.5	0594	0.2663
(WAXS+EXAFS method)	0.4	0786	0.1250
	0.3	0885	0.0845
	0.2	0966	0.0619
	0.1	1157	0.0411
$Cu_{26}As_{37}Se_{37}$		0000	3.5810
	0.5	0634	0.5341
(WAXS+EXAFS method)	0.4	0798	0.3435
	0.3	0887	0.2882
	0.2	1143	0.0716
	0.1	1504	0.0459

TABLE IV. Thermal isotropic factor (σ_j) refining process for each alloy.

Sample	Coord. sphere	r_{min} (Å)	r_{max} (Å)	σ_j^2 (Å^2)
$Cu_8As_{26}Se_{66}$	1st	0.0	3.0	0.0002
	2nd	3.0	4.9	0.0031
(WAXS method)	3rd	4.9	6.5	0.0224
	4th	6.5	8.2	0.0384
	5th	8.2	12.0	0.0107
$Cu_{26}As_{37}Se_{37}$	1st	0.0	3.0	0.0002
	2nd	3.0	5.0	0.0057
(WAXS method)	3rd	5.0	6.6	0.0103
	4th	6.6	8.4	0.0446
	5th	8.4	12.0	0.0535

a least-squares iterative method, for the WAXS RDF constraints only. Table IV summarizes the coordination spheres of the RDF with the best-fit temperature factors. It is given in order to show their coupling and the deviations compatible with the model. Also a similar set of values (not shown) was obtained, for the simulation of the model owing to the WAXS RDF plus EXAFS constraints. Once the thermal factor refining process was finished, the quadratic deviations between the theoretical and experimental values of $rG(r)$ were reduced for both simulations assays to the values shown in Table V. The model is compatible with WAXS data and WAXS+EXAFS data as both fittings are acceptable, having the WAXS+EXAFS-based model with a bigger standard deviation because the modeling is more constrained as movements breaking the local order required by EXAFS analysis are not allowed. The model indicates the more probable structure from a statistical point of view is not unique at a local level.

Once the refining process has terminated, the resulting atomic configuration is used to obtain the model's reduced RDF and interference function and to discuss the main structural parameters. In Fig. 3 we compare along the same axis the reduced RDF obtained from the spatial model against the experimental ones for samples *L* and *H*, in the case of simulation based on WAXS RDF plus EXAFS, a good match can be observed.

With the aim of showing the agreement between the simulated model and experimental data, and of looking for some topological features in the medium-range order, we calculated the inverse Fourier transform to obtain the model's reduced interference function (Fig. 4). The fitting between the experimental and modeled interference function is satisfactory but does not reproduce the first sharp diffraction peak observed in the WAXS RDF of the *H* sample, and does so only slightly for the *L* sample.

TABLE V. Quadratic deviations (ε^2) between theoretical and experimental values of $rG(r)$, for both modeling approaches.

Sample	WAXS-RDF	WAXS+EXAFS	ε^2
$Cu_8As_{26}Se_{66}$	x		0.0305
$Cu_{26}As_{37}Se_{37}$	x		0.0312
$Cu_8As_{26}Se_{66}$		x	0.0401
$Cu_{26}As_{37}Se_{37}$		x	0.0452

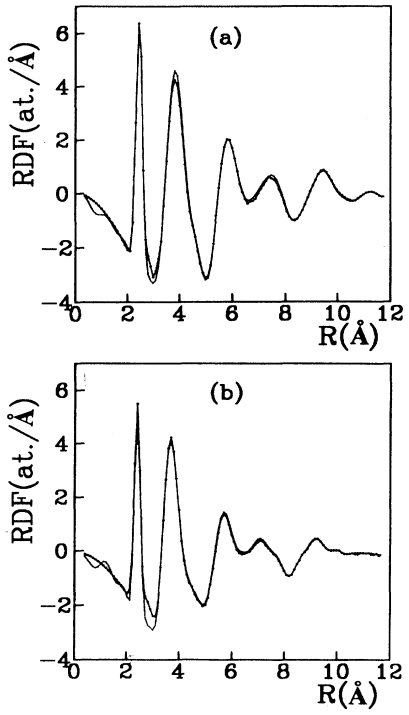

FIG. 3. Plot agreement between the experimental and modeled (pointed line) reduced radial distribution function (a) for the $Cu_{26}As_{37}Se_{37}$ alloy and (b) for the $Cu_8As_{26}Se_{66}$ alloy.

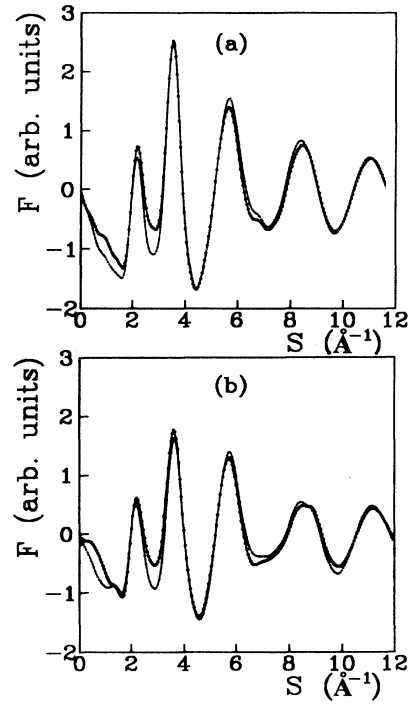

FIG. 4. Plot of agreement between the experimental and modeled (pointed line) reduced interference function (a) for the $Cu_8As_{37}Se_{37}$ alloy and (b) for the $Cu_8As_{26}Se_{66}$ alloy.

TABLE VI. Coordinations (N) and pair distances (d) reached in the models from WAXS method and combined WAXS+EXAFS method.

Sample	Pair	N (WAXS)	d (Å) (WAXS)	N (WAXS+EXAFS)	d (Å) (WAXS+EXAFS)
$Cu_8As_{26}Se_{66}$	Cu-Cu				
	Cu-As	0.30	2.40	0.20	2.42
	Cu-Se	2.80	2.40	3.10	2.41
	As-Cu	0.09	2.40	0.06	2.42
	As-As	0.97	2.42	0.33	2.41
	As-Se	1.24	2.41	2.12	2.40
	Se-Cu	0.33	2.40	0.37	2.41
	Se-As	0.49	2.41	0.88	2.40
	Se-Se	1.23	2.41	0.71	2.39
$Cu_{26}As_{37}Se_{37}$	Cu-Cu	1.07	2.43	0.28	2.47
	Cu-As	1.23	2.42	0.74	2.42
	Cu-Se	1.56	2.44	2.30	2.45
	As-Cu	0.86	2.42	0.59	2.42
	As-As	0.96	2.42	0.59	2.41
	As-Se	0.80	2.42	1.44	2.44
	Se-Cu	1.10	2.44	1.62	2.45
	Se-As	0.79	2.42	1.44	2.44
	Se-Se	0.99	2.42	0.17	2.42

From the model's atomic position arrangement, the coordination distances d and pair distribution statistics N can be obtained. Table VI shows the WAXS RDF modeling simulation coordination (third and fourth columns), and WAXS-EXAFS results when both were taken at the same time (fifth and sixth columns). The simulation results can be compared with the fifth and sixth columns from Table I. The lower values of the fifth columns against the corresponding values in Table I are logical as the simulated model has a finite radius and therefore reveals the atoms with unsaturated atoms near the periphery. The distance bond lengths are close to those obtained in the EXAFS experiment, except for the Cu-Se pair, which are compatible with the values found in the literature.

IV. CONCLUSIONS

The accuracy of the sample generation and obtaining the RDF has been verified by a double assay with one of the studied samples. The structural SRO parameter derived from WAXS RDF analysis is a condition satisfied by the structural parameter reached in the EXAFS spectroscopic study of our sample.

A modified modeling MC simulation technique has been implemented, taking into account the structural information of both WAXS and EXAFS. The models satisfy the coordination and pair distance requirements and give a fine-tuned set of pair distances. In addition, as a feasible result, the inverse Fourier transform of the model's RDF for both samples agrees well with the experimental SRO information and even describes some topological aspects of medium-range order for one of them. Nevertheless the ε^2 factor is worth in the case of WAXS+EXAFS assays due to the increased number of constraints imposed in the numerical process.

ACKNOWLEDGMENTS

We appreciate very much the interesting discussion with H. Dexpert, and V. Mastelaro from LURE, and we thank the staff in charge of the DCI machine for the allocation of the beam line.

[1]A. C. Adams, *Plasma Deposited Thin Films,* edited by J. Mort and F. Jansen (CRC, Boca Raton, 1986).

[2]J. Chang, Tetsji Yano, Astuo Yasumori, Masayuki Yamane, and J. D. Mackenzie, *Sixth International Workshop on Glasses and Ceramics from Gels, DP6,* edited by L. Esquivias (University of Cádiz, Sevilla, 1991).

[3]K. S. Liang, A. Bienenstock, and C. W. Bates, Phys. Rev. B **10**, 1529 (1974).

[4]M. M. Haifz, M. M. Ibrahim, M. M. Dongol, and F. H. Hammad, J. Appl. Phys. **54**, 1950 (1983).

[5]N. Mott and E. A. Davis, *Electronic Processes in Non-Crystalline Materials,* 2nd ed. (Clarendon, Oxford, 1979).

[6]S. Neov, M. Baeva, I. Gerassmore, and M. Nikiforova, Phys. Status Solidi A **57**, 795 (1980).

[7]J. Z. Liu and P. C. Taylor, Solid State Commun. **70**, 81 (1989).

[8]N. de la Rosa-Fox, L. Esquivias, P. Villares, and R. Jimenez-Garay, Phys. Rev. B **33**, 4094 (1986).

[9]Z. U. Borisova, *Glassy Semiconductors* (Plenum, New York, 1981).

[10]C. Prieto, P. Lagarde, H. Dexpert, V. Briois, F. Villain, and M. Verdaguer, Meas. Sci. Technol. **3**, 325 (1992).

[11]B. E. Warren, *X-Ray Diffraction* (Addison-Wesley, Reading, MA, 1969).

[12]A. D. Anjou and F. Sanz, J. Non-Cryst. Solids **28**, 319 (1978).

[13]J. C. Phillips, Phys. Status Solidi B **101**, 473 (1980).
[14]J. M. Conejo, N. De la Rosa-Fox, L. Esquivias, and R. Jimenez-Garay, Mater. Lett. **4**, 11 (1986).
[15]D. Gomez, L. Esquivias, and C. Prieto, *Actas 3ª Reunion Nacional de Ciencia de Materiales,* edited by I. Carrizosa *et al.* (ICMS-CSIC, Sevilla, 1990).
[16]B. K. Teo, *EXAFS Principles and Data Analysis. Inorganic Chemistry Concepts Vol. 9* (Springer-Verlag, Berlin, 1986).
[17]A. G. Mckale, B. W. Veal, A. P. Paulikas, S. K. Chan, and G. S. Kanpp, J. Am. Chem. Soc. **110**, 3763 (1988).
[18]D. Gomez, L. Esquivias, and C. Prieto, Phys. Status Solidi B **169**, 303 (1992).
[19]E. O. Brigham, in *The Fast Fourier Transform* (Prentice-Hall, New York, 1971).
[20]S. H. Hunter, A. Bienenstock, and T. M. Hayes, *Proceedings of the 7th International Conference on Amorphous Liquid Semiconductors,* edited by W. E. Spear (University of Edinburgh, Edinburgh, 1977).
[21]Z. M. Saleh, G. A. Williams, and P. C. Taylor, J. Non-Cryst. Solids **114**, 58 (1989).
[22]J. Z. Liu and P. C. Taylor, J. Non-Cryst. Solids **114**, 25 (1989).
[23]L. Esquivias and F. Sanz, J. Non-Cryst. Solids **70**, 221 (1985).
[24]J. Vazquez, P. Villares, E. Marquez, and R. Jimenez-Garay, Mater. Chem. Phys. **25**, 399 (1990).
[25]G. Mason, Nature (London) **217**, 733 (1968).